

Schizophrenia risk from complex variation of complement component 4

Aswin Sekar^{1,2,3}, Allison R. Bialas^{4,5}, Heather de Rivera^{1,2}, Avery Davis^{1,2}, Timothy R. Hammond⁴, Nolan Kamitaki^{1,2}, Katherine Tooley^{1,2}, Jessy Presumey⁵, Matthew Baum^{1,2,3,4}, Vanessa Van Doren¹, Giulio Genovese^{1,2}, Samuel A. Rose², Robert E. Handsaker^{1,2}, Schizophrenia Working Group of the Psychiatric Genomics Consortium*, Mark J. Daly^{2,6}, Michael C. Carroll⁵, Beth Stevens^{2,4} & Steven A. McCarroll^{1,2}

Schizophrenia is a heritable brain illness with unknown pathogenic mechanisms. Schizophrenia's strongest genetic association at a population level involves variation in the major histocompatibility complex (MHC) locus, but the genes and molecular mechanisms accounting for this have been challenging to identify. Here we show that this association arises in part from many structurally diverse alleles of the complement component 4 (*C4*) genes. We found that these alleles generated widely varying levels of *C4A* and *C4B* expression in the brain, with each common *C4* allele associating with schizophrenia in proportion to its tendency to generate greater expression of *C4A*. Human *C4* protein localized to neuronal synapses, dendrites, axons, and cell bodies. In mice, *C4* mediated synapse elimination during postnatal development. These results implicate excessive complement activity in the development of schizophrenia and may help explain the reduced numbers of synapses in the brains of individuals with schizophrenia.

Schizophrenia is a heritable psychiatric disorder involving impairments in cognition, perception, and motivation that usually manifest late in adolescence or early in adulthood. The pathogenic mechanisms underlying schizophrenia are unknown, but observers have repeatedly noted pathological features involving excessive loss of grey matter^{1,2}, and reduced numbers of synaptic structures on neurons^{3–5}. Although treatments exist for the psychotic symptoms of schizophrenia, there is no mechanistic understanding of, nor effective therapies to prevent or treat, the cognitive impairments and deficit symptoms of schizophrenia, which are the earliest and most constant features of the disorder. An important goal in human genetics is to find the biological processes that underlie such disorders.

More than 100 loci in the human genome contain single nucleotide polymorphism (SNP) haplotypes that associate with risk of schizophrenia⁶; however, the functional alleles and mechanisms at these loci remain to be discovered. By far the strongest such genetic relationship is schizophrenia's association with genetic markers across the major histocompatibility complex (MHC) locus, which spans several megabases (Mb) of chromosome 6 (refs 6–10). The MHC locus is best known for its role in immunity, containing 18 highly polymorphic human leukocyte antigen (*HLA*) genes that encode a vast suite of antigen-presenting molecules. In some autoimmune diseases, genetic associations at the MHC locus arise from alleles of *HLA* genes^{11,12}; however, schizophrenia's association to the MHC has not yet been explained.

Though the functional alleles that give rise to genetic associations have in general been challenging to find, the schizophrenia–MHC association has been particularly challenging because schizophrenia's complex pattern of association to markers in the MHC locus spans hundreds of genes and does not correspond to the linkage disequilibrium (LD) around any known variant^{6,10}. This prompted us to consider cryptic genetic influences that might generate unconventional genetic signals. The most strongly associated markers in

several large case/control cohorts were near a complex, multi-allelic, and only partially characterized form of genome variation that affects the *C4* gene encoding complement component 4 (Extended Data Fig. 1). The association of schizophrenia to *CSMD1* (refs 6, 10), which encodes a regulator of *C4* (ref. 13), further motivated us to consider *C4*.

C4 structures and MHC SNP haplotypes

Human *C4* exists as two functionally distinct genes (isotypes), *C4A* and *C4B*; both vary in structure and copy number. One to three *C4* genes (*C4A* and/or *C4B*) are commonly present as a tandem array within the MHC class III region (Fig. 1a and Extended Data Fig. 1g)^{14–18}. The protein products of *C4A* and *C4B* bind different molecular targets^{19,20}. *C4A* and *C4B* segregate in both long (L) and short (S) genomic forms (*C4AL*, *C4AS*, *C4BL* and *C4BS*), distinguished by the presence or absence (in intron 9) of a human endogenous retroviral (HERV) insertion that lengthens *C4* from 14 to 21 kb without changing the *C4* protein sequence¹⁶ (Fig. 1b).

We developed a way (Extended Data Fig. 2) to identify the 'structural haplotypes' of *C4*—the copy number of *C4A* and *C4B* and the long/short (HERV) status of each *C4A* and *C4B* copy—present on 222 copies of human chromosome 6. Using droplet digital PCR (ddPCR), we found that genomes contained 0–5 *C4A* genes, 0–3 *C4B* genes, 1–5 long (L) *C4* genes, and 0–3 short (S) *C4* genes (Extended Data Fig. 2a, b). We also developed assays to determine the long/short (HERV) status of each *C4A* and *C4B* gene copy (Extended Data Fig. 2c), thus revealing copy number of *C4AL*, *C4BL*, *C4AS*, and *C4BS* in each genome (Supplementary Methods).

We analysed inheritance in father–mother–offspring trios (Extended Data Fig. 2d) to identify the *C4A* and *C4B* contents of individual alleles (Extended Data Fig. 2e). We found that four common *C4* structural haplotypes (AL–BL, AL–BS, AL–AL, and BS) were collectively present

¹Department of Genetics, Harvard Medical School, Boston, Massachusetts 02115, USA. ²Stanley Center for Psychiatric Research, Broad Institute of MIT and Harvard, Cambridge, Massachusetts 02142, USA. ³MD-PhD Program, Harvard Medical School, Boston, Massachusetts 02115, USA. ⁴Department of Neurology, F.M. Kirby Neurobiology Center, Boston Children's Hospital, Harvard Medical School, Boston, Massachusetts 02115, USA. ⁵Program in Cellular and Molecular Medicine, Boston Children's Hospital, Boston, Massachusetts 02115, USA. ⁶Analytical and Translational Genetics Unit, Massachusetts General Hospital, Boston, Massachusetts 02114, USA.

*Lists of participants and their affiliations appear in the Supplementary Information.

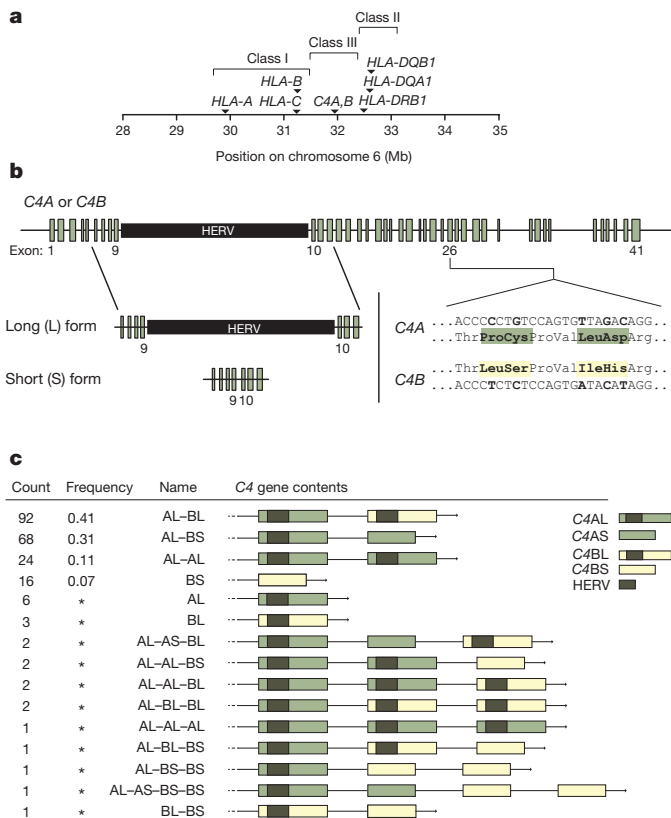


Figure 1 | Structural variation of the complement component 4 (C4) gene. **a**, Location of the C4 genes within the major histocompatibility complex (MHC) locus on human chromosome 6. **b**, Human C4 exists as two paralogous genes (isotypes), C4A and C4B; the encoded proteins are distinguished at a key site that determines which molecular targets they bind^{19,20}. Both C4A and C4B also exist in both long (L) and short (S) forms distinguished by an endogenous retroviral (C4-HERV) sequence in intron 9. **c**, Structural forms of the C4 locus and their frequencies among a European-ancestry population sample (222 chromosomes from 111 genetically unrelated individuals, HapMap CEU), inferred as described in Extended Data Fig. 2. Asterisks indicate allele frequencies too low to be estimated accurately.

on 90% of the 222 independent chromosomes sampled; 11 uncommon C4 haplotypes comprised the other 10% (Fig. 1c).

The series of many SNP alleles along a genomic segment (the SNP haplotype) can be used to identify chromosomal segments that come from shared common ancestors. We identified the SNP haplotype(s) on which each C4 locus structure was present (Fig. 2). The three most common C4 locus structures were each present on multiple MHC SNP haplotypes (Fig. 2). For example, the C4 AL-BS structure (frequency 31%) was present on five common haplotypes (frequencies 4%, 4%, 4%, 8%, and 6%) and many rare haplotypes (collective frequency 5%, Fig. 2). Reflecting this haplotype diversity, each of these C4 structures exhibited real but only partial correlation to individual SNPs (Extended Data Fig. 3). The relationship between C4 structures and SNP haplotypes was generally one-to-many: a C4 structure might be present on many haplotypes, but a given SNP haplotype tended to have one characteristic C4 structure (Fig. 2).

C4 expression variation in the brain

As C4A and C4B vary in both copy number and C4-HERV status (Fig. 1), and because other HERVs can function as enhancers^{21–23}, C4 variation might affect expression of C4 genes. We assessed how C4 structural variation related to RNA expression of C4A and C4B in eight panels of post-mortem human adult brain samples (674 samples from 245 distinct donors in 3 cohorts, Supplementary Methods).

The results of this expression analysis were consistent across all five brain regions analysed. First, RNA expression of C4A and C4B increased proportionally with copy number of C4A and C4B respectively (Fig. 3a, b and Extended Data Fig. 4). These observations mirror earlier observations in human serum²⁴. Second, expression levels of C4A were two to three times greater than expression levels of C4B, even after controlling for relative copy number in each genome (Fig. 3c). Third, copy number of the C4-HERV sequence increased the ratio of C4A to C4B expression ($P < 10^{-7}$, $P < 10^{-2}$, $P < 10^{-3}$, respectively, in the three cohorts examined, by Spearman rank correlation) (Fig. 3c and Extended Data Fig. 4).

We used the above data to create genetic predictors of C4A and C4B expression levels in the brain (Supplementary Methods). If C4A or C4B expression levels influence a phenotype, then the aggregate genetic predictor might associate to schizophrenia more strongly than individual variants do.

C4 structural variation in schizophrenia

Schizophrenia cases and controls from 22 countries have been analysed genome-wide for SNPs, implicating the MHC locus as the strongest of more than 100 genome-wide-significant associations⁶. Our analysis indicated that long haplotypes defined by many SNPs carry characteristic C4 alleles (Fig. 2), potentially making it possible to infer C4 alleles by statistical imputation²⁵ from combinations of many SNPs. We used our 222 integrated haplotypes of MHC SNPs and C4 alleles (Fig. 2) as reference chromosomes for imputation. We found that the four most common structural forms of the C4A/C4B locus (BS, AL-BS, AL-BL, and AL-AL) could be inferred with reasonably high accuracy (generally $0.70 < r^2 < 1.00$, Supplementary Table 2).

We then analysed SNP data from 28,799 schizophrenia cases and 35,986 controls, from 40 cohorts in 22 countries contributing to the Psychiatric Genomics Consortium (PGC)⁶. We evaluated association to 7,751 SNPs across the extended MHC locus (chr6: 25–34 Mb), to C4 structural alleles (Fig. 1c), and to HLA sequence polymorphisms imputed from the SNP data. We also predicted levels of C4A and C4B expression from the imputed C4 structural alleles.

The association of schizophrenia to these genetic variants exhibited two prominent features (Fig. 4a, b). One feature involved a large set of similarly associating SNPs spanning 2 Mb across the distal end of the extended MHC region (we use this set's most strongly associating SNP, rs13194504, as its genetic proxy). The other peak of association centred at C4, where schizophrenia associated most strongly with the genetic predictor of C4A expression levels ($P = 3.6 \times 10^{-24}$) (Fig. 4a and Extended Data Fig. 5). In the region near C4 (chromosome 6, 31–33 Mb), the more strongly a SNP correlated with predicted C4A expression, the more strongly it associated with schizophrenia (Fig. 4b, bottom panel).

Although the variation at C4 and in the distal extended MHC region associated with schizophrenia with similar strengths ($P = 3.6 \times 10^{-24}$ and 5.5×10^{-28} , respectively), their correlation with each other was low ($r^2 = 0.18$, Fig. 4b), suggesting that they reflect distinct genetic influences. Conditional analysis confirmed this: in analyses controlling for either rs13194504 or genetically predicted C4A expression, the other genetic variable still defined a genome-wide-significant association peak ($P = 7.8 \times 10^{-10}$ and 8.0×10^{-14} , respectively, Fig. 4c, d). Controlling for both genetic variables revealed a third association signal just proximal to the MHC locus (Fig. 4e) involving SNPs around BAK1 and SYNGAP1, the latter of which encodes a major component of the postsynaptic density; *de novo* loss-of-function mutations in SYNGAP1 associate with autism²⁶. In joint analysis, all three genetic signals remained significant ($P = 8.0 \times 10^{-14}$, 2.8×10^{-8} , and 1.7×10^{-8} , respectively) and no additional genome-wide-significant signals remained in the MHC locus (Fig. 4f).

In some autoimmune diseases with genetic associations in the MHC locus, alleles of HLA genes associate more strongly than do other variants in the MHC locus, appearing to explain the associations^{11,12}. In contrast, in schizophrenia, classical HLA alleles

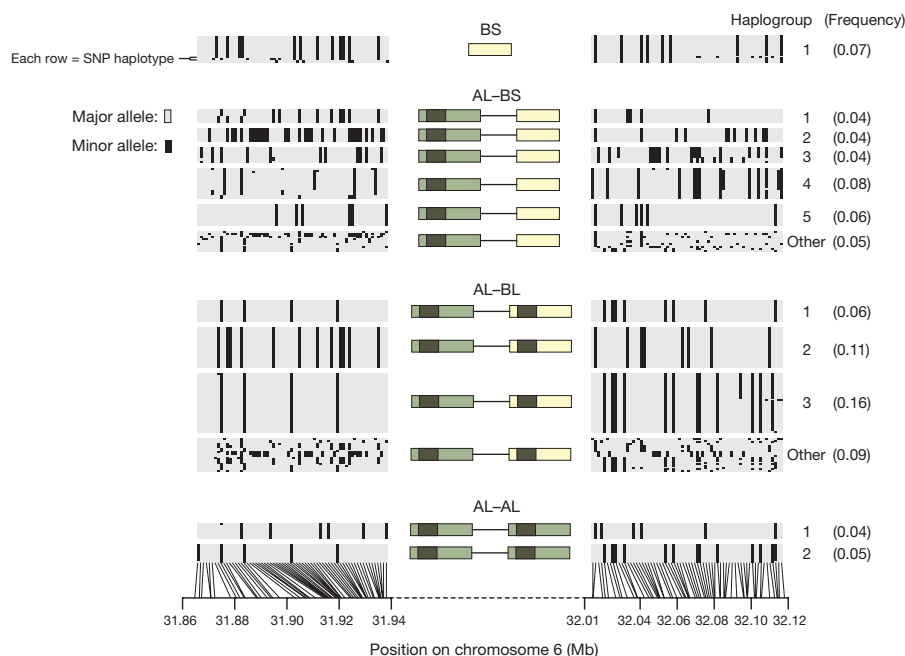


Figure 2 | Haplotypes formed by *C4* structures and SNPs. SNP haplotype(s) on which common *C4* structures were present. Each thin horizontal line represents the series of SNP alleles (haplotype) along a 250 kilobase (kb) chromosomal segment. Each column represents a SNP; grey and black indicate which allele is present on each haplotype. The SNP

haplotypes are grouped into 13 sets of haplotypes associating with each of the four most common *C4* structures. Three *C4* structures (AL-BS, AL-BL, and AL-AL) each segregated on multiple SNP haplotypes (numbered at right).

associated with schizophrenia less strongly than other genetic variants in the MHC region did (Extended Data Fig. 6). We further considered the strongest schizophrenia associations to classical *HLA* alleles at distinct loci (involving *HLA-B*0801*, *HLA-DRB1*0301*, and *HLA-DQB1*02*); conditional analysis indicated that each could be explained by LD to the stronger signals at *C4* and rs13194504 (Extended Data Fig. 7).

If each *C4* allele affects schizophrenia risk via its effect on *C4A* expression, then this relationship should be visible across specific *C4* alleles. We measured schizophrenia risk levels for the common *C4* structural alleles (BS, AL-BS, AL-BL, and AL-AL); these alleles showed relative risks ranging from 1.00 to 1.27 (Fig. 5a). We also estimated (from the post-mortem brain samples) the *C4A* expression levels generated by these four alleles (Fig. 5b). Schizophrenia risk and *C4A* expression levels yielded the same ordering of the *C4* allelic series (Fig. 5a, b).

We sought an even more stringent test. If this allelic series of relationships with schizophrenia risk (Fig. 5a) arises from *C4* locus structure—rather than from other genetic variation in the MHC locus—then a given *C4* structure should exhibit the same schizophrenia risk regardless of the MHC haplotype on which it appears. We measured the schizophrenia association of all 13 common combinations of *C4* structure and MHC SNP haplotype (Fig. 5c). Across this allelic series, each *C4* allele exhibited a characteristic level of schizophrenia risk, regardless of the haplotype on which it was present (Fig. 5c).

C4A RNA expression in schizophrenia

These genetic findings (Fig. 5a, c) predict that *C4A* expression might be elevated in brain tissue from schizophrenia patients. We measured *C4A* RNA expression levels in brain tissue from 35 schizophrenia patients and 70 individuals without schizophrenia. The median expression of *C4A* in brain tissues from schizophrenia patients was 1.4-fold greater ($P = 2 \times 10^{-5}$ by Mann-Whitney *U*-test; Fig. 5d) and was elevated in each of the five brain regions assayed (Extended Data Fig. 8). This relationship did not meaningfully change in analyses adjusted for age or post-mortem interval. The relationship remained significant after correcting for the higher average *C4A* copy number among the brain donors affected with schizophrenia (1.3-fold greater, $P = 0.002$). Some earlier studies have also reported elevated levels of complement proteins in serum of schizophrenia patients^{27,28}.

C4 in the central nervous system

C4 is a critical component of the classical complement cascade, an innate immune system pathway that rapidly recognizes and eliminates pathogens and cellular debris. In the brain, other genes in the classical complement cascade have been implicated in the elimination or ‘pruning’ of synapses^{29–31}.

To evaluate the distribution of *C4* in human brain, we performed immunohistochemistry on sections of the prefrontal cortex and hippocampus. We observed *C4*⁺ cells in the grey and white matter, with the greatest number of *C4*⁺ cells detected in the hippocampus. Co-staining with cell-type-specific markers revealed *C4* in subsets of NeuN⁺ neurons (Fig. 6a; antibody specificity further evaluated in

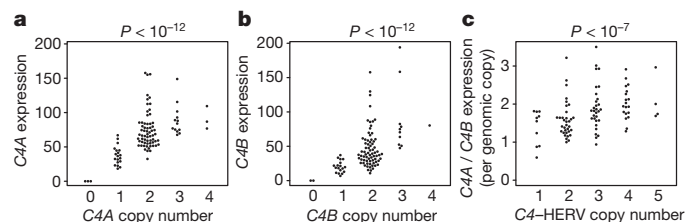


Figure 3 | Brain RNA expression of *C4A* and *C4B* in relation to copy numbers of *C4A*, *C4B*, and the *C4-HERV*. a, b, mRNA expression of *C4A* (a) and *C4B* (b) was measured (by ddPCR) in brain tissue from 244 individuals. The copy numbers of *C4A*, *C4B*, and the *C4-HERV* were measured (by ddPCR) in genomic DNA from the brain donors. The results were consistent across 8 panels of brain tissue representing 5 brain regions and 3 distinct sets of donors (one set shown here, with data from 101 individuals; all panels in Extended Data Fig. 4; a few outlier points are beyond the range of these plots but are shown in Extended Data Fig. 4). *P* values were obtained by a Spearman rank correlation test. In c, expression of *C4A* (per genomic copy) is normalized to expression of *C4B* (per genomic copy) to control for *trans*-acting influences shared by *C4A* and *C4B*.

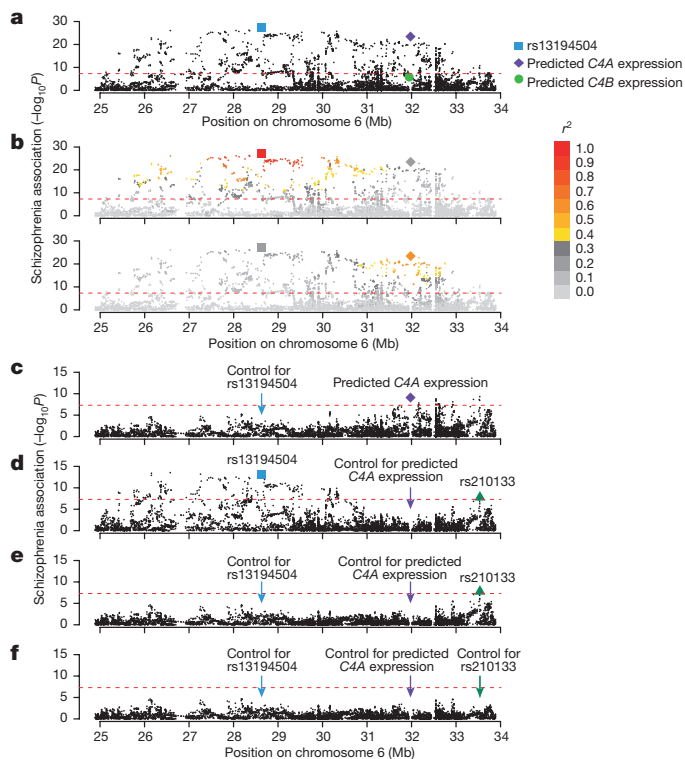


Figure 4 | Association of schizophrenia to *C4* and the extended MHC locus. Association of schizophrenia to 7,751 SNPs across the MHC locus and to genetically predicted expression levels of *C4A* and *C4B* in the brain (represented in the genomic location of the *C4* gene). The data shown are based on analysis of 28,799 schizophrenia cases and 35,986 controls of European ancestry from the Psychiatric Genomics Consortium. The height of each point represents the statistical strength ($-\log_{10}(P)$) of association with schizophrenia. **a, b**, Association of schizophrenia to SNPs in the MHC locus and to genetically predicted expression of *C4A* and *C4B*. In **b**, genetic variants are coloured by their levels of correlation to rs13194504 (upper panel) or by their levels of correlation to genetically predicted brain *C4A* expression levels (lower panel). **c–f**, Conditional association analysis. The red dashed line indicates the statistical threshold for genome-wide significance ($P = 5 \times 10^{-8}$). See also Extended Data Figs 5–7 for detailed association analyses involving *C4* locus structures and *HLA* alleles.

Extended Data Fig. 9a) and a subset of astrocytes. Much of the *C4* immunoreactivity was punctate (Fig. 6b), co-localizing with synaptic puncta identified by co-immunostaining for the pre- and postsynaptic markers VGLUT1/2 (also known as SLC17A7 and SLC17A6, respectively) and PSD-95 (also known as DLG4) (Fig. 6b). These results suggest that *C4* is produced by, or deposited on, neurons and synapses.

To further characterize neuronal *C4*, we cultured human primary cortical neurons and evaluated *C4* expression, localization, and secretion. Neurons expressed *C4* mRNA and secreted *C4* protein (Extended Data Fig. 9c). Neurons exhibited *C4*-immunoreactive puncta along their processes and cell bodies (Fig. 6c, d; antibody specificity further evaluated in Extended Data Fig. 9b). About 75% of *C4* immunoreactivity localized to neuronal processes (Fig. 6c); of the *C4* in neuronal processes, approximately 65% was observed in dendrites (MAP2⁺, neurofilament⁺ processes) and 35% in axons (MAP2[−], neurofilament⁺ processes). Punctate *C4* immunoreactivity was observed at 48% of structural synapses as defined by co-localized synaptotagmin and PSD-95 (Fig. 6d).

The association of increased *C4* with schizophrenia (Figs 4 and 5), the presence of *C4* at synapses (Fig. 6b, d), the involvement of other complement proteins in synapse elimination^{29–31}, and earlier reports of decreased synapse numbers in schizophrenia patients^{3–5}, together suggested that *C4* might work with other components of the classical complement cascade to promote synaptic pruning. To test this hypothesis,

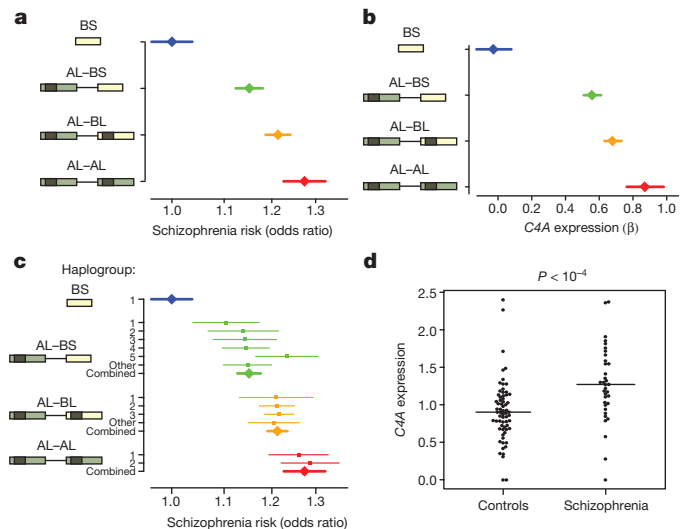


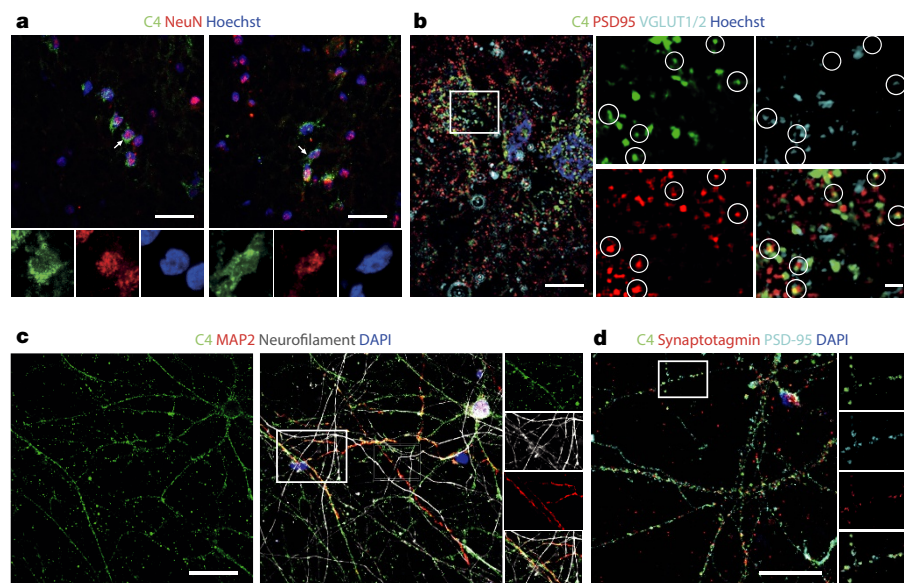
Figure 5 | *C4* structures, *C4A* expression, and schizophrenia risk. **a**, Schizophrenia risk associated with four common structural forms of *C4* in analysis of 28,799 schizophrenia cases and 35,986 controls. **b**, Brain *C4A* RNA expression levels associated with four common structural forms of *C4*. β was calculated from fitting *C4A* RNA expression (in brain tissue) to the number of chromosomes (0, 1, or 2) carrying each *C4* structure (across 120 individuals sampled). **c**, Schizophrenia risk associated with 13 combinations of *C4* structural allele and MHC SNP haplotype. The numbers on the y axis adjacent to the *C4* structures indicate the ‘haplogroup’, the MHC SNP haplotype background on which the *C4* structure segregates, and correspond to Fig. 2. Statistical tests of heterogeneity yielded $P = 0.55$ for AL–AL alleles; $P = 0.93$ for AL–BL alleles; $P = 0.06$ for AL–BS alleles; and $P = 5.7 \times 10^{-5}$ across the overall allelic series. **d**, Expression levels of *C4A* RNA were directly measured (by RT-ddPCR) in post-mortem brain samples from 35 schizophrenia patients and 70 individuals not affected with schizophrenia. Measurements for all five brain regions analysed exhibited the same relationship (Extended Data Fig. 8). Horizontal lines show the median value for each group. P values were derived by a (non-parametric) one-sided Mann–Whitney test. Error bars shown in **a–c** represent 95% confidence intervals around the effect size estimate.

we moved to a mouse model. *C4A* and *C4B* appear to have functionally specialized outside the rodent lineage, but the mouse genome contains a *C4* gene that shares features with both *C4A* and *C4B* (Extended Data Fig. 10a, b). Impairments in schizophrenia tend to affect higher cognitive functions and recently expanded brain regions for which analogies in mice are uncertain³². However, waves of postnatal synapse elimination occur in many brain regions, and strong experimental models have been established in several mammalian visual systems. In these systems, synaptic projections from retinal ganglion cells (RGCs) onto thalamic relay neurons within the dorsal lateral geniculate nucleus (dLGN) of the visual thalamus undergo activity-dependent synaptic refinement^{29–31,33–35}. We found that *C4* RNA was expressed in the LGN and in RGCs purified from the retina during the period of synaptic pruning (Extended Data Fig. 10c).

In the immune system, *C4* promotes C3 activation, allowing C3 to covalently attach onto its targets and promote their engulfment by phagocytic cells. In the developing mouse brain, C3 targets subsets of synapses and is required for synapse elimination by microglia, the principal CNS cells expressing receptors for complement^{29,30}. We found that in mice deficient in *C4* (ref. 36), C3 immunostaining in the dLGN was greatly reduced compared to wild-type littermates (Fig. 7a, b), with fewer synaptic inputs being C3-positive in the absence of *C4* (Fig. 7c). These data demonstrate a role for *C4* in complement deposition on synaptic inputs.

We then evaluated whether mice deficient in *C4* had defects in synaptic remodelling, as has been described for C3-deficient mice²⁹. Mice lacking functional *C4* exhibited greater overlap between RGC inputs from the two eyes ($P < 0.001$) than wild-type littermate controls,

Figure 6 | C4 protein at neuronal cell bodies, processes and synapses. **a**, C4 protein localization in human brain tissue. Two representative confocal images (drawn from immunohistochemistry performed on samples from five individuals with schizophrenia and two unaffected individuals) within the hippocampal formation demonstrate localization of C4 in a subset of NeuN⁺ neurons. **b**, High-resolution structured illumination microscopy (SIM) imaging of tissue in the hippocampal formation reveals colocalization of C4 with the presynaptic terminal markers VGLUT1/2 and the postsynaptic marker PSD-95. **c**, Confocal images of primary human cortical neurons show colocalization of C4, MAP2, and neurofilament along neuronal processes. **d**, Confocal image of primary cortical neurons stained for C4, presynaptic marker synaptotagmin, and postsynaptic marker PSD-95. Scale bars, 25 μ m (**a**, **c**, and **d**); 5 μ m (**b**, left); and 1 μ m (**b**, right). Extended Data Fig. 9 contains additional data on antibody specificity.



suggesting reduced synaptic pruning (Fig. 7d, Extended Data Fig. 10d, e, and Supplementary Methods). The degree of deficit in $C4^{-/-}$ mice was similar to that previously reported for $C1q^{-/-}$ and

$C3^{-/-}$ mice^{29,31}. Heterozygous $C4^{+/-}$ mice, with one wild-type copy of C4, had an intermediate phenotype (Fig. 7d). These data provide direct evidence that C4 mediates synaptic refinement in the developing brain.

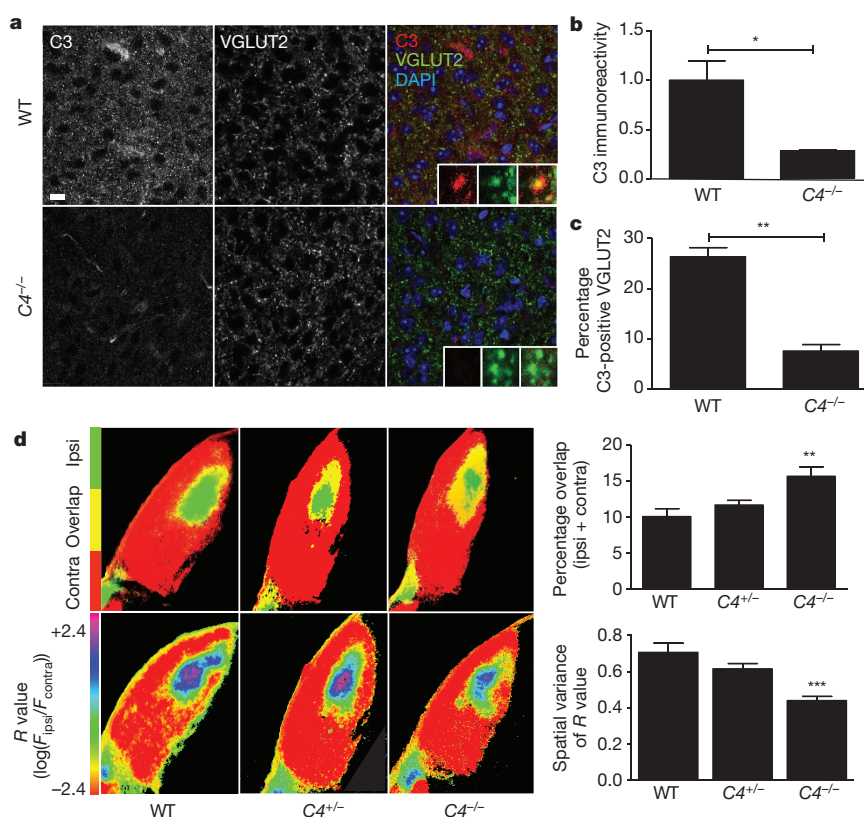


Figure 7 | C4 in retinogeniculate synaptic refinement. **a**, Representative confocal images of immunohistochemistry for C3 in the P5 dLGN showed reduced C3 deposition in the dLGN of $C4^{-/-}$ mice compared to wild-type (WT) littermates. **b**, Quantification confirmed reduced C3 immunoreactivity in the dLGN ($n = 3$ mice per group, $P < 0.05$, t -test; y axis: mean fluorescence intensity, normalized to wild type). **c**, Co-localization analysis revealed a reduction in the fraction of VGLUT2⁺ puncta that were C3⁺ in $C4$ -deficient mice relative to their WT littermates ($n = 3$ mice per group, $P = 0.0011$, two-sided t -test). **d**, Synaptic refinement in mice with 0, 1, or 2 copies of C4. These images represent the segregation of ipsilateral and contralateral RGC projections to the dLGN; two analysis methods were used. Top, projections from

the ipsilateral (green) and contralateral (red) eyes show minimal overlap (yellow) in wild-type mice. The overlapping area is significantly increased in $C4^{-/-}$ mice ($n = 6$ mice per group, $P < 0.01$, ANOVA with Bonferroni post-hoc tests). Bottom, threshold-independent analysis using the R value⁵⁰ ($R = \log_{10}(F_{\text{ipsi}}/F_{\text{contra}})$). Pixels are pseudocoloured with an R value heat map (red indicates areas having only contralateral inputs; purple, only ipsilateral inputs). Compared to their wild-type littermates, $C4$ -deficient mice exhibited lower R value variance, indicating defects in synaptic refinement ($n = 6$ mice per group, $P < 0.001$, ANOVA with Bonferroni post-hoc tests). Control experiments analysing total dLGN size, dLGN area receiving ipsilateral input, and number of RGCs are shown in Extended Data Fig. 10f–h, respectively. Error bars in **b–d** represent s.e.m.

Discussion

We developed ways to analyse a complex form of genome structural variation (Figs 1 and 2) and discovered that schizophrenia's association with variation in the MHC locus involves many common, structurally distinct *C4* alleles that affect expression of *C4A* and *C4B* in the brain; each allele associated with schizophrenia risk in proportion to its effect on *C4A* expression (Figs 3–5). We found that *C4* is expressed by neurons, localized to dendrites, axons, and synapses, and is secreted (Fig. 6). In mice, *C4* promoted synapse elimination during the developmentally timed maturation of a neuronal circuit (Fig. 7).

In humans, adolescence and early adulthood bring extensive elimination of synapses in distributed association regions of cerebral cortex, such as the prefrontal cortex, that have greatly expanded in recent human evolution and appear to become impaired in schizophrenia^{37–40}. Synapse elimination in human association cortex appears to continue from adolescence into the third decade of life³⁹. This late phase of cortical maturation, which may distinguish humans even from some other primates³⁷, corresponds to the period during which schizophrenia most often becomes clinically apparent and patients' cognitive function declines, a temporal correspondence that others have also noted⁴¹.

The principal pathological findings in brains of those affected with schizophrenia involve loss of cortical grey matter without cell death: affected individuals exhibit abnormal cortical thinning^{1,2} and reduced numbers of synaptic structures on cortical pyramidal neurons^{3–5}. In the brain, complement receptors are expressed primarily by microglia, the phagocytic immune cells of the central nervous system. The possibility that neuron–microglia interactions via the complement cascade contribute to schizophrenia pathogenesis—for example, that schizophrenia arises or intensifies from excessive or inappropriate synaptic pruning by microglia during adolescence and early adulthood—would offer a potential mechanism for these longstanding observations about age of onset and synapse loss. Many other genetic findings in schizophrenia involve genes that encode synaptic proteins^{6,42–44}. Diverse synaptic abnormalities could in principle interact with the complement system and other pathways^{45,46} to cause excessive stimulation of microglia and elimination of synapses during adolescence and early adulthood.

The two human *C4* genes (*C4A* and *C4B*) exhibited distinct relationships with schizophrenia risk, with increased risk associating most strongly with variation that increases expression of *C4A*. Human *C4A* and *C4B* proteins, whose functional specialization appears to be evolutionarily recent (Extended Data Fig. 10a), show striking biochemical differences: *C4A* more readily forms amide bonds with proteins, while *C4B* favours binding to carbohydrate surfaces^{19,20}, differences with an established basis in *C4* protein sequence and structure^{47,48}. An intriguing possibility is that *C4A* and *C4B* differ in affinity for an unknown binding site at synapses.

To date, few genome-wide association study (GWAS) associations have been explained by specific functional alleles. An unexpected finding at *C4* involves the large number of common, functionally distinct forms of the same locus that appear to contribute to schizophrenia risk. The human genome contains hundreds of other genes with complex, multi-allelic forms of structural variation⁴⁹. It will be important to learn the extent to which such variation contributes to brain diseases and to all human phenotypes.

Online Content Methods, along with any additional Extended Data display items and Source Data, are available in the online version of the paper; references unique to these sections appear only in the online paper.

Received 19 May; accepted 18 December 2015.

Published online 27 January 2016.

1. Cannon, T. D. *et al.* Cortex mapping reveals regionally specific patterns of genetic and disease-specific gray-matter deficits in twins discordant for schizophrenia. *Proc. Natl Acad. Sci. USA* **99**, 3228–3233 (2002).
2. Cannon, T. D. *et al.* Progressive reduction in cortical thickness as psychosis develops: a multisite longitudinal neuroimaging study of youth at elevated clinical risk. *Biol. Psychiatry* **77**, 147–157 (2015).
3. Garey, L. J. *et al.* Reduced dendritic spine density on cerebral cortical pyramidal neurons in schizophrenia. *J. Neurol. Neurosurg. Psychiatry* **65**, 446–453 (1998).

4. Glantz, L. A. & Lewis, D. A. Decreased dendritic spine density on prefrontal cortical pyramidal neurons in schizophrenia. *Arch. Gen. Psychiatry* **57**, 65–73 (2000).
5. Glausier, J. R. & Lewis, D. A. Dendritic spine pathology in schizophrenia. *Neuroscience* **251**, 90–107 (2013).
6. Schizophrenia Working Group of the Psychiatric Genomics Consortium. Biological insights from 108 schizophrenia-associated genetic loci. *Nature* **511**, 421–427 (2014).
7. Shi, J. *et al.* Common variants on chromosome 6p22.1 are associated with schizophrenia. *Nature* **460**, 753–757 (2009).
8. Stefansson, H. *et al.* Common variants conferring risk of schizophrenia. *Nature* **460**, 744–747 (2009).
9. International Schizophrenia Consortium *et al.* Common polygenic variation contributes to risk of schizophrenia and bipolar disorder. *Nature* **460**, 748–752 (2009).
10. Schizophrenia Psychiatric Genome-Wide Association Study Consortium. Genome-wide association study identifies five new schizophrenia loci. *Nature Genet.* **43**, 969–976 (2011).
11. Howson, J. M., Walker, N. M., Clayton, D. & Todd, J. A. Confirmation of HLA class II independent type 1 diabetes associations in the major histocompatibility complex including HLA-B and HLA-A. *Diabetes Obes. Metab.* **11** (Suppl 1), 31–45 (2009).
12. Raychaudhuri, S. *et al.* Five amino acids in three HLA proteins explain most of the association between MHC and seropositive rheumatoid arthritis. *Nature Genet.* **44**, 291–296 (2012).
13. Escudero-Esparza, A., Kalchishkova, N., Kurbasic, E., Jiang, W. G. & Blom, A. M. The novel complement inhibitor human CUB and Sushi multiple domains 1 (CSMD1) protein promotes factor I-mediated degradation of C4b and C3b and inhibits the membrane attack complex assembly. *FASEB J.* **27**, 5083–5093 (2013).
14. Carroll, M. C., Campbell, R. D., Bentley, D. R. & Porter, R. R. A molecular map of the human major histocompatibility complex class III region linking complement genes *C4*, *C2* and factor *B*. *Nature* **307**, 237–241 (1984).
15. Carroll, M. C., Belt, T., Palsdottir, A. & Porter, R. R. Structure and organization of the *C4* genes. *Phil. Trans. R. Soc. Lond. B* **306**, 379–388 (1984).
16. Dangel, A. W. *et al.* The dichotomous size variation of human complement *C4* genes is mediated by a novel family of endogenous retroviruses, which also establishes species-specific genomic patterns among Old World primates. *Immunogenetics* **40**, 425–436 (1994).
17. Horton, R. *et al.* Variation analysis and gene annotation of eight MHC haplotypes: the MHC Haplotype Project. *Immunogenetics* **60**, 1–18 (2008).
18. Bánlák, Z., Doleschall, M., Rajczy, K., Fust, G. & Szilagyi, A. Fine-tuned characterization of RCCX copy number variants and their relationship with extended MHC haplotypes. *Genes Immun.* **13**, 530–535 (2012).
19. Law, S. K., Dodds, A. W. & Porter, R. R. A comparison of the properties of two classes, *C4A* and *C4B*, of the human complement component *C4*. *EMBO J.* **3**, 1819–1823 (1984).
20. Isenman, D. E. & Young, J. R. The molecular basis for the difference in immune hemolysis activity of the Chido and Rodgers isotypes of human complement component *C4*. *J. Immunol.* **132**, 3019–3027 (1984).
21. Illarionova, A. E., Vinogradova, T. V. & Sverdlov, E. D. Only those genes of the KIAA1245 gene subfamily that contain HERV(K) LTRs in their introns are transcriptionally active. *Virology* **358**, 39–47 (2007).
22. Nakamura, A., Okazaki, Y., Sugimoto, J., Oda, T. & Jinno, Y. Human endogenous retroviruses with transcriptional potential in the brain. *J. Hum. Genet.* **48**, 575–581 (2003).
23. Suntsova, M. *et al.* Human-specific endogenous retroviral insert serves as an enhancer for the schizophrenia-linked gene *PRODH*. *Proc. Natl Acad. Sci. USA* **110**, 19472–19477 (2013).
24. Yang, Y. *et al.* Diversity in intrinsic strengths of the human complement system: serum *C4* protein concentrations correlate with *C4* gene size and polygenic variations, hemolytic activities, and body mass index. *J. Immunol.* **171**, 2734–2745 (2003).
25. Browning, S. R. & Browning, B. L. Rapid and accurate haplotype phasing and missing-data inference for whole-genome association studies by use of localized haplotype clustering. *Am. J. Hum. Genet.* **81**, 1084–1097 (2007).
26. Iossifov, I. *et al.* The contribution of *de novo* coding mutations to autism spectrum disorder. *Nature* **515**, 216–221 (2014).
27. Mayilyan, K. R., Arnold, J. N., Presanis, J. S., Soghoyan, A. F. & Sim, R. B. Increased complement classical and mannan-binding lectin pathway activities in schizophrenia. *Neurosci. Lett.* **404**, 336–341 (2006).
28. Hakobyan, S., Boyajyan, A. & Sim, R. B. Classical pathway complement activity in schizophrenia. *Neurosci. Lett.* **374**, 35–37 (2005).
29. Stevens, B. *et al.* The classical complement cascade mediates CNS synapse elimination. *Cell* **131**, 1164–1178 (2007).
30. Schafer, D. P. *et al.* Microglia sculpt postnatal neural circuits in an activity and complement-dependent manner. *Neuron* **74**, 691–705 (2012).
31. Bialas, A. R. & Stevens, B. TGF- β signaling regulates neuronal C1q expression and developmental synaptic refinement. *Nature Neurosci.* **16**, 1773–1782 (2013).
32. Kaiser, T. & Feng, G. Modeling psychiatric disorders for developing effective treatments. *Nature Med.* **21**, 979–988 (2015).
33. Shatz, C. J. & Kirkwood, P. A. Prenatal development of functional connections in the cat's retinogeniculate pathway. *J. Neurosci.* **4**, 1378–1397 (1984).
34. Sretavan, D. W. & Shatz, C. J. Prenatal development of retinal ganglion cell axons: segregation into eye-specific layers within the cat's lateral geniculate nucleus. *J. Neurosci.* **6**, 234–251 (1986).

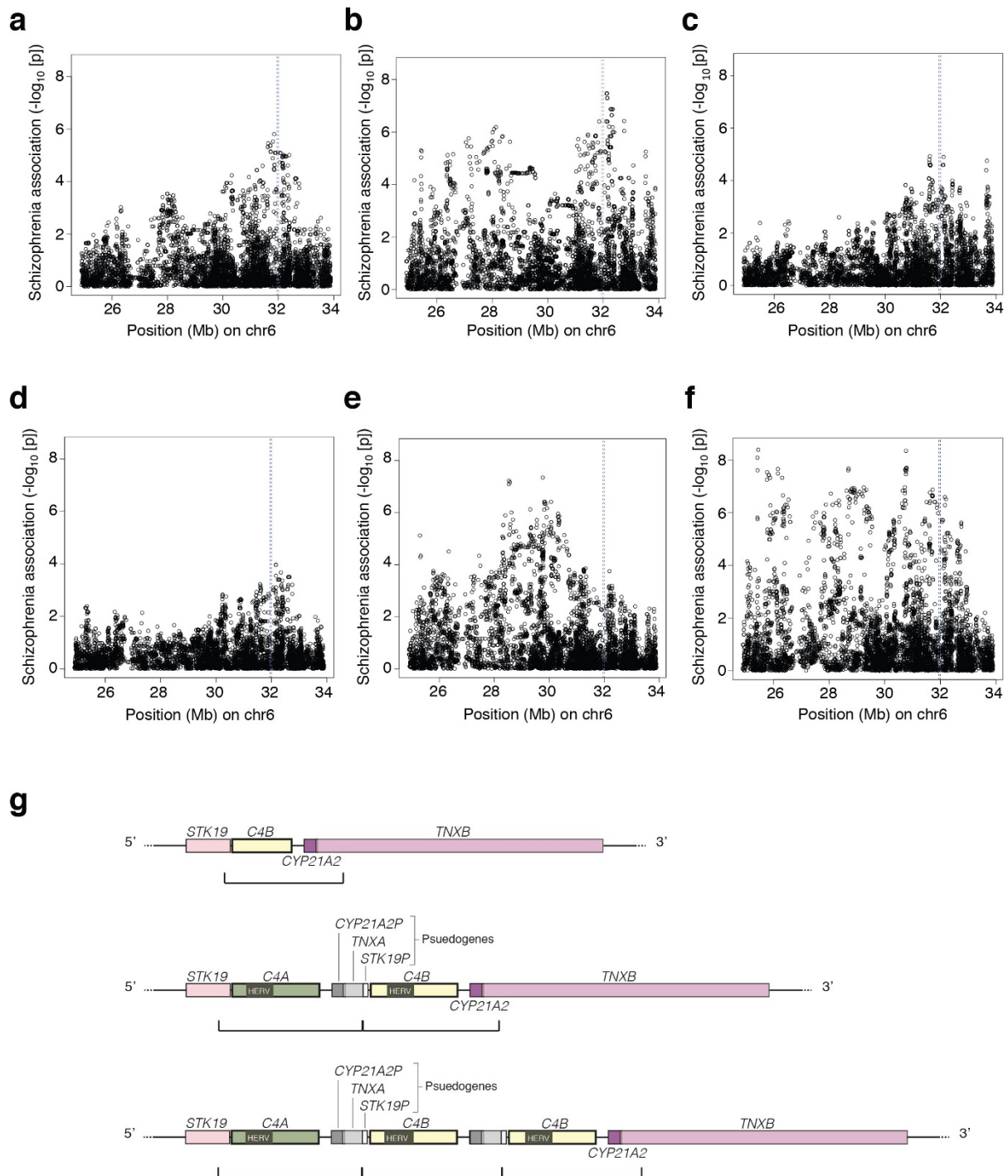
35. Chen, C. & Regehr, W. G. Developmental remodeling of the retinogeniculate synapse. *Neuron* **28**, 955–966 (2000).
36. Fischer, M. B. *et al.* Regulation of the B cell response to T-dependent antigens by classical pathway complement. *J. Immunol.* **157**, 549–556 (1996).
37. Huttenlocher, P. R. & Dabholkar, A. S. Regional differences in synaptogenesis in human cerebral cortex. *J. Comp. Neurol.* **387**, 167–178 (1997).
38. Huttenlocher, P. R. Synaptic density in human frontal cortex—developmental changes and effects of aging. *Brain Res.* **163**, 195–205 (1979).
39. Petanjek, Z. *et al.* Extraordinary neoteny of synaptic spines in the human prefrontal cortex. *Proc. Natl Acad. Sci. USA* **108**, 13281–13286 (2011).
40. Buckner, R. L. & Krienen, F. M. The evolution of distributed association networks in the human brain. *Trends Cogn. Sci.* **17**, 648–665 (2013).
41. Feinberg, I. Schizophrenia: caused by a fault in programmed synaptic elimination during adolescence? *J. Psychiatr. Res.* **17**, 319–334 (1982–1983).
42. Kirov, G. *et al.* *De novo* CNV analysis implicates specific abnormalities of postsynaptic signalling complexes in the pathogenesis of schizophrenia. *Mol. Psychiatry* **17**, 142–153 (2012).
43. Fromer, M. *et al.* *De novo* mutations in schizophrenia implicate synaptic networks. *Nature* **506**, 179–184 (2014).
44. Purcell, S. M. *et al.* A polygenic burden of rare disruptive mutations in schizophrenia. *Nature* **506**, 185–190 (2014).
45. Datwani, A. *et al.* Classical MHCI molecules regulate retinogeniculate refinement and limit ocular dominance plasticity. *Neuron* **64**, 463–470 (2009).
46. Lee, H. *et al.* Synapse elimination and learning rules co-regulated by MHC class I H2-Db. *Nature* **509**, 195–200 (2014).
47. van den Elsen, J. M. *et al.* X-ray crystal structure of the C4d fragment of human complement component C4. *J. Mol. Biol.* **322**, 1103–1115 (2002).
48. Dodds, A. W., Ren, X. D., Willis, A. C. & Law, S. K. The reaction mechanism of the internal thioester in the human complement component C4. *Nature* **379**, 177–179 (1996).
49. Handsaker, R. E. *et al.* Large multiallelic copy number variations in humans. *Nature Genet.* **47**, 296–303 (2015).
50. Torborg, C. L. & Feller, M. B. Unbiased analysis of bulk axonal segregation patterns. *J. Neurosci. Methods* **135**, 17–26 (2004).
51. Fernando, M. M. *et al.* Assessment of complement C4 gene copy number using the paralog ratio test. *Hum. Mutat.* **31**, 866–874 (2010).
52. Rudduck, C., Beckman, L., Franzen, G., Jacobsson, L. & Lindstrom, L. Complement factor C4 in schizophrenia. *Hum. Hered.* **35**, 223–226 (1985).
53. Schroers, R. *et al.* Investigation of complement C4B deficiency in schizophrenia. *Hum. Hered.* **47**, 279–282 (1997).
54. Mayilyan, K. R., Dodds, A. W., Boyajyan, A. S., Soghoyan, A. F. & Sim, R. B. Complement C4B protein in schizophrenia. *World J. Biol. Psychiatry* **9**, 225–230 (2008).
55. Jia, X. *et al.* Imputing amino acid polymorphisms in human leukocyte antigens. *PLoS ONE* **8**, e64683 (2013).
56. Nonaka, M., Nakayama, K., Yeul, Y. D. & Takahashi, M. Complete nucleotide and derived amino acid sequences of sex-limited protein (Slp), nonfunctional isotype of the fourth component of mouse complement (C4). *J. Immunol.* **136**, 2989–2993 (1986).

Supplementary Information is available in the online version of the paper.

Acknowledgements The authors would like to remember the late T. Stanley with appreciation and express their gratitude for his support. We thank S. Hyman, E. Lander, C. Bargmann, and C. Patil for conversations about the project and comments on drafts of the manuscript; M. Webster for expert advice on immunohistochemistry; B. Browning for expert advice on imputation; the Stanley Medical Research Institute Brain Collection and the NHGRI Gene and Tissue Expression (GTEx) Project for access to RNA and tissue samples; C. Emba for assistance with experiments; and C. Usher for contributions to manuscript figures. This work was supported by R01 HG 006855 (to S.A.M.), by the Stanley Center for Psychiatric Research (to S.A.M. and B.S.), by U01 MH105641 (to S.A.M.), by R01 MH077139 (to the PGC), and by T32 GM007753 (to A.S. and M.B.).

Author Contributions S.A.M. and A.S. conceived the genetic studies. A.S. performed the laboratory experiments and computational analyses to understand the molecular and population genetics of the C4 locus (Figs 1 and 2). A.S., K.T., N.K., and V.V.D. analysed C4 expression variation in human brain (Figs 3 and 5b, d). G.G., R.E.H., and S.A.R. contributed to genetic analyses. A.S. and A.D. did the imputation and association analysis (Figs 4 and 5a, c). M.J.D. provided advice on the association analyses. Investigators in the Schizophrenia Working Group of the Psychiatric Genomics Consortium collected and phenotyped cohorts and contributed genotype data for analysis. B.S. and M.C.C. contributed expertise and reagents for experiments described in Fig. 6 and 7. H.d.R. and T.R.H. performed the C4 immunocytochemistry and immunohistochemistry experiments respectively, with advice from A.R.B. (Fig. 6). A.R.B. and J.P. analysed the role of C4 in synaptic refinement in the mouse visual system (Fig. 7). M.B. analysed C4 expression in mice. S.A.M. and A.S. wrote the manuscript with contributions from all authors.

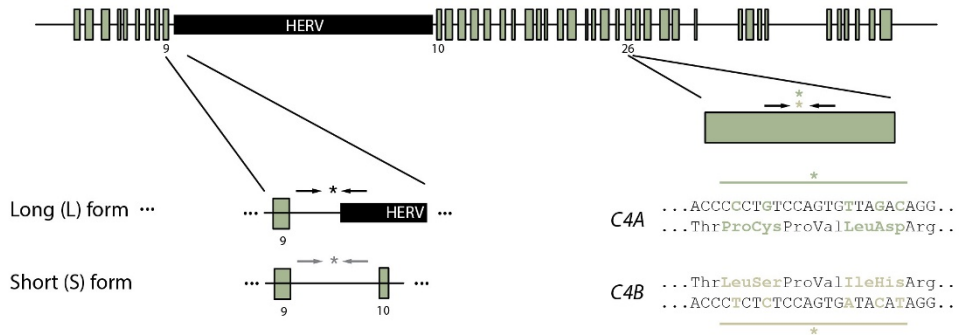
Author Information Reprints and permissions information is available at www.nature.com/reprints. The authors declare no competing financial interests. Readers are welcome to comment on the online version of the paper. Correspondence and requests for materials should be addressed to S.A.M. (mccarroll@genetics.med.harvard.edu).



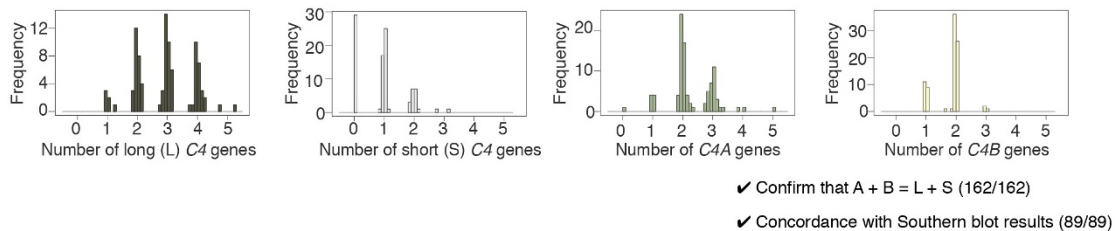
Extended Data Figure 1 | Association of schizophrenia to common variants in the MHC locus in individual case-control cohorts, and schematic of the repeat module containing C4. **a–f,** Data for several schizophrenia case-control cohorts that were genome-scanned before we began this work (**a–d**) exhibits peaks of association near chr6: 32 Mb (blue vertical line) on the human genome reference sequence (GRCh37/hg19). Note that association patterns vary from cohort to cohort, reflecting statistical sampling fluctuations and potentially fluctuations in allele frequencies of the (unknown) causal variants in different cohorts. Cohorts such as in **b, e** and **f** suggest the existence of effects at multiple loci within the MHC region. Even in the cohorts with simpler peaks (**a, c, d**), the pattern of association across the individual SNPs at chr6: 32 Mb does not correspond to the LD around any known variant. This motivated the focus in the current work on cryptic genetic influences in this region that could cause unconventional association signals that do not resemble the LD patterns of individual variants. **g.** A complex form of genome structural variation resides near chr6:

32 Mb. Shown here are three of the known alternative structural forms of this genomic region. The most prominent feature of this structural variation is the tandem duplication of a genomic segment that contains a C4 gene, 3' fragments of the STK19 and TNXB genes, and a pseudogenized copy of the CYP21A2 gene. This cassette is present in 1–3 copies on the three alleles depicted above; the boundaries below each haplotype demarcate the sequence that is duplicated. Haplotypes with multiple copies of this module (middle and bottom) contain multiple functional copies of C4, whereas the additional gene fragments or copies denoted STK19P, CYP21A2P, and TNXA are typically pseudogenized. Rare haplotypes with a gain or loss of intact CYP21A2 have also been observed¹⁸. Although C4A and C4B contain multiple sequence variants, they are defined based on the differences encoded by exon 26, which determine the relative affinities of C4A and C4B for distinct molecular targets^{19,20} (Fig. 1). Many additional forms of this locus appear to have arisen by non-allelic homologous recombination and gene conversion (ref. 18 and Fig. 1).

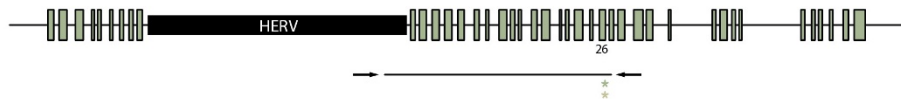
- a** Molecular assays to measure the copy number of each *C4* gene type (A or B isotype; long or short form) in each genome sampled.



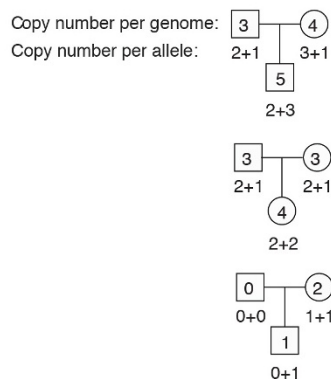
- b** Measure copy number of each *C4* gene type in 162 individuals' genomes (from HapMap).



- c** Molecular assays to measure the copy number of compound structural forms of *C4* (e.g. *C4AL*).



- d** Use inheritance in trios to infer copy number on shared and unshared chromosomal copies.

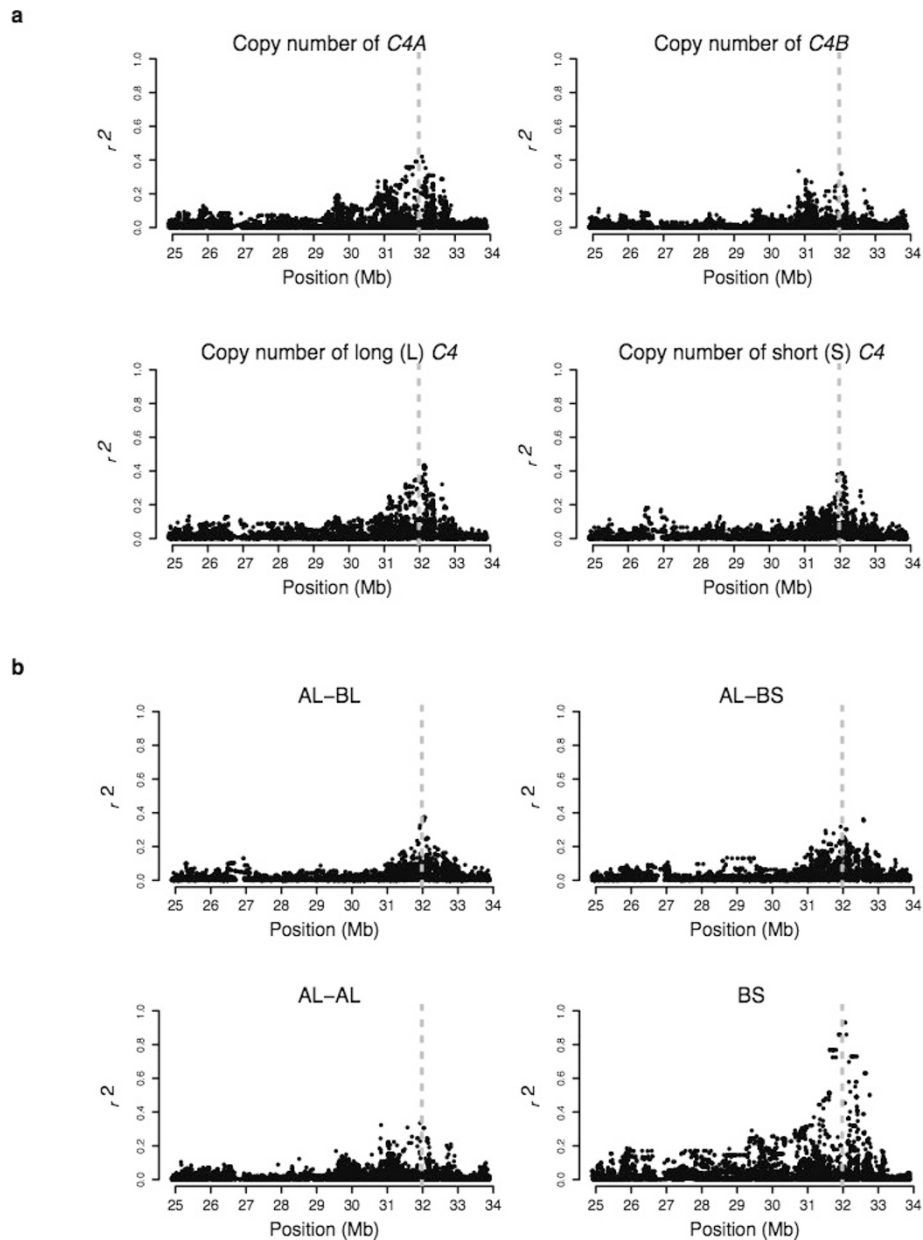


- e** Infer the *C4* gene contents of the founder chromosomes in each trio. Where possible, use existing sequence data to also infer gene order.



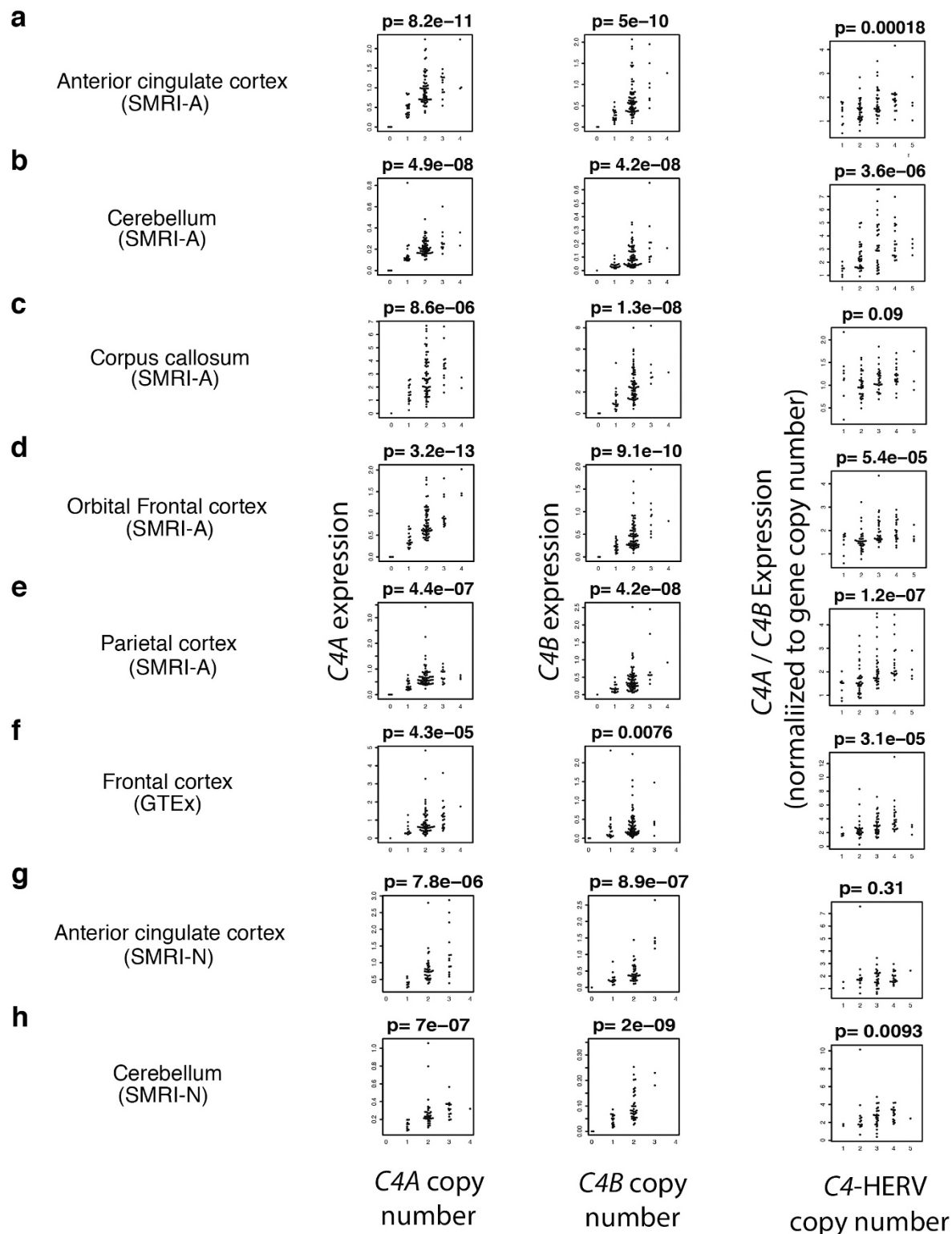
Extended Data Figure 2 | Schematic of strategy for identifying the segregating structural forms of the *C4* locus. **a**, Molecular assays for measuring copy number of the key, variable *C4* structural features—the length polymorphism (HERV insertion) that distinguishes the long (L) from the short (S) genomic form of *C4*, and the *C4A/C4B* isotypic difference. Each primer–probe–primer assay is represented with the combination of arrows (primers) and asterisk (probe) in its approximate genomic location (though not to scale). **b**, Measurement of copy number of *C4* gene types in the genomes of 162 individuals (from HapMap CEU sample). The absolute, integer copy number of each *C4* gene type in each genome is precisely inferred from the resulting data. To ensure high accuracy, the data are further evaluated for a checksum relationship ($A + B = L + S$) and for concordance with earlier data from Southern blotting of 89 of the same HapMap individuals⁵¹. **c**, To measure the copy

number of compound structural forms of *C4* (involving combinations of L/S and A/B), we perform long-range PCR followed by quantitative measurement of the A/B isotype-distinguishing sequences in droplets. **d**, Analysis of transmissions in father–mother–offspring trios enables inference of the *C4* gene contents of individual copies (alleles) of chromosome 6. Three example trios are shown in this schematic. **e**, Examples of the inferred structural forms of the *C4* locus (more shown in Fig. 1c). For the common *C4* structures (AL–BL, AL–BS, AL–AL, and BS), genomic order of the *C4* gene copies is known from earlier assemblies of sequence contigs in individuals homozygous for MHC haplotypes due to consanguinity¹⁷ and other molecular analyses of the *C4* locus¹⁸. For the rarer *C4* structures, the genomic order of *C4* gene copies is hypothesized or provisional.



Extended Data Figure 3 | Linkage disequilibrium relationships (r^2) of MHC SNPs to forms of C4 structural variation. a, b, Correlations of SNPs in the MHC locus with copy number of C4 gene types (a) and larger-scale structural forms (haplotypes) (b) of the C4 locus. Dashed,

vertical lines indicate the genomic location of the C4 locus. C4 structural forms show only partial correlation (r^2) to the allelic states of nearby SNPs, reflecting the relationship shown in Fig. 2, in which a structural form of the C4 locus often segregates on multiple different SNP haplotypes.



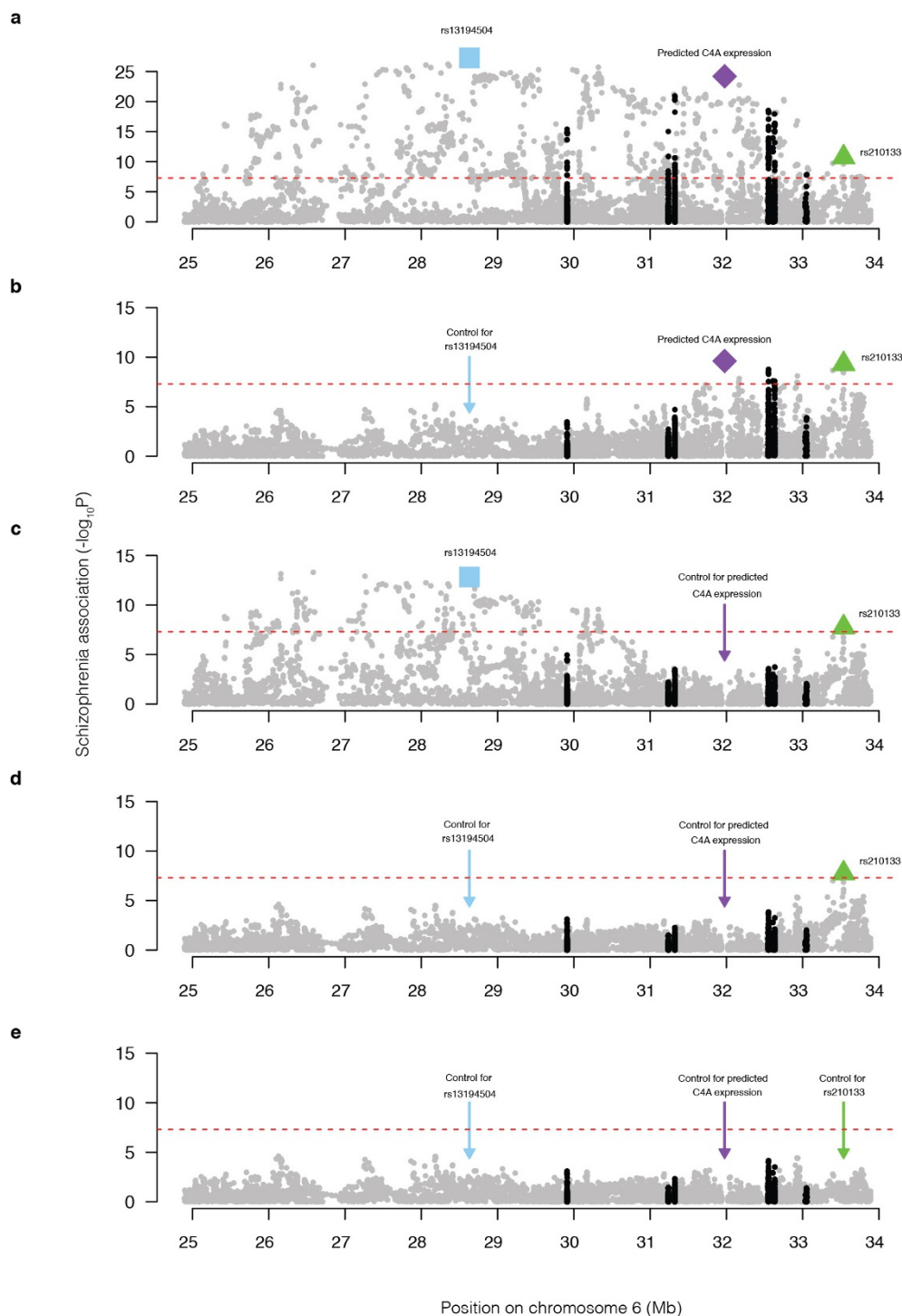
Extended Data Figure 4 | RNA expression of *C4A* and *C4B* in relation to copy number of *C4A*, *C4B*, and the *C4*-HERV (long form of *C4*), in eight panels of post-mortem brain tissue. Copy number of *C4* structural features was measured by ddPCR; RNA expression levels were measured by RT-ddPCR. **a–e**, Data for tissues from the Stanley Medical Research Institute (SMRI) Array Consortium consisting of anterior cingulate cortex (**a**), cerebellum (**b**), corpus callosum (**c**), orbital frontal cortex (**d**), and parietal cortex (**e**). **f**, Data for the frontal cortex samples from the NHGRI Genes and Tissues Expression (GTEx) Project. **g, h**, Data for tissues from the SMRI Neuropathology Consortium (anterior cingulate cortex and cerebellum, respectively). These data were then used to inform (by linear

regression) the derivation of a linear model for predicting each individual's RNA expression of *C4A* and *C4B* as a function of the numbers of copies of AL, BL, AS, and BS. The derivation of this model, and the regression coefficients induced, are described in Supplementary Methods. In the rightmost plot of each panel, expression of *C4A* (per genomic copy) is normalized to expression of *C4B* (per genomic copy) to more specifically visualize the effect of the *C4*-HERV by controlling for genomic copy number and for any *trans*-acting influences shared by *C4A* and *C4B*; the inferred regression coefficients (Supplementary Methods) suggest that the observed effect is mostly due to increased expression of *C4A*.

	Association of SCZ with this variant (unconditioned analysis)			Association of SCZ with this variant (joint analysis with predicted <i>C4A</i> expression as a covariate)			Association of SCZ with genetically predicted <i>C4A</i> expression (joint analysis with this variant as a covariate)		
	p	β	SE	p	β	SE	p	β	SE
Expression predictors (derived from <i>post mortem</i> brain RNA analysis)									
<i>C4A</i> expression (genetic prediction from imputed <i>C4</i> locus structure)	3.60E-24	0.247	0.024	NA	NA	NA	NA	NA	NA
<i>C4B</i> expression (genetic prediction from imputed <i>C4</i> locus structure)	2.31E-07	-0.092	0.018	0.71	0.008	0.021	2.35E-18	0.253	0.029
Copy number of <i>C4</i> structural features									
<i>C4A</i> genes	6.31E-19	0.112	0.013	0.45	-0.023	0.030	6.54E-07	0.287	0.058
<i>C4B</i> genes	1.45E-04	-0.066	0.017	0.63	0.009	0.019	4.58E-21	0.252	0.027
Long <i>C4</i> genes (with HERV)	7.09E-23	0.084	0.009	0.17	0.029	0.021	4.89E-03	0.170	0.060
Short <i>C4</i> genes (no HERV)	3.94E-14	-0.085	0.011	0.32	-0.015	0.015	7.38E-12	0.225	0.033
Total <i>C4</i> copy number	9.41E-15	0.123	0.016	1.00	0.000	0.025	5.40E-11	0.247	0.038
Specific <i>C4</i> locus structures (haplotypes of one or more <i>C4</i> genes)									
BS	2.29E-19	-0.171	0.019	0.16	-0.045	0.032	1.10E-06	0.200	0.041
AL-BS	0.03	-0.027	0.013	0.62	0.007	0.013	3.39E-23	0.250	0.025
AL-BL	6.16E-07	0.058	0.012	0.41	0.011	0.013	6.34E-19	0.238	0.027
AL-AL	2.09E-06	0.093	0.020	0.56	-0.013	0.023	2.49E-19	0.256	0.028
Combinations of <i>C4</i> locus structure and flanking SNP haplotype									
AL-BS-4	0.21	-0.027	0.022	0.95	-0.002	0.022	7.99E-24	0.247	0.025
AL-BS-2	0.35	-0.031	0.033	0.80	-0.008	0.033	5.45E-24	0.247	0.024
AL-BS-3	0.34	-0.028	0.029	0.91	-0.003	0.030	5.69E-24	0.247	0.024
AL-BS-5	0.07	0.053	0.029	0.01	0.077	0.029	5.73E-25	0.252	0.024
AL-BS-1	0.04	-0.064	0.031	0.19	-0.040	0.031	1.32E-23	0.245	0.024
AL-BS-other	0.30	-0.023	0.022	0.92	0.002	0.023	6.19E-24	0.247	0.025
AL-BL-2	0.03	0.036	0.017	0.77	0.005	0.017	3.52E-23	0.246	0.025
AL-BL-3	2.15E-03	0.042	0.014	0.55	0.008	0.014	3.28E-22	0.243	0.025
AL-BL-1	0.35	0.032	0.034	0.92	0.003	0.035	5.55E-24	0.247	0.024
AL-BL-other	0.23	0.029	0.024	0.95	0.002	0.024	7.37E-24	0.247	0.025
AL-AL-1	0.01	0.074	0.028	0.38	-0.026	0.029	9.42E-23	0.255	0.026
AL-AL-2	3.33E-04	0.097	0.027	0.94	-0.002	0.029	2.31E-21	0.248	0.026
Alternative hypotheses									
<i>C4B</i> nulls (for whom total <i>C4B</i> copy number = 0) *	0.36	0.061	0.066						

Extended Data Figure 5 | Detailed analysis of the association of schizophrenia to genetic variation at and around *C4*, in data from 28,799 schizophrenia cases and 35,986 controls. (Psychiatric Genomics Consortium, ref. 6.) SCZ, schizophrenia; β, estimated effect size per copy of the genomic feature or allele indicated; SE, standard error. Detailed association analyses of *HLA* alleles are in Extended Data Figs 6 and 7. The single asterisk (*) indicates that we specifically tested *C4B*-null status because a 1985 study⁵² reported an analysis of 165 schizophrenia patients

and 330 controls in which rare *C4B*-null status associated with elevated risk of schizophrenia, though two subsequent studies^{53,54} found no association of schizophrenia to *C4B*-null genotype. We sought to evaluate this using the large data set in this study, finding no association to *C4B*-null status. The double asterisk (**) indicates total copy number of *C4* is also strongly correlated to copy number of the *CYP21A2P* pseudogene, which is present on duplicated copies of the sequence shown in Extended Data Fig. 1g.



Extended Data Figure 6 | Evaluation of the association of schizophrenia with *HLA* alleles and coding-sequence polymorphisms. **a–e**, Associations to *HLA* alleles and coding-sequence polymorphisms are shown in black; to provide the context of levels of association to

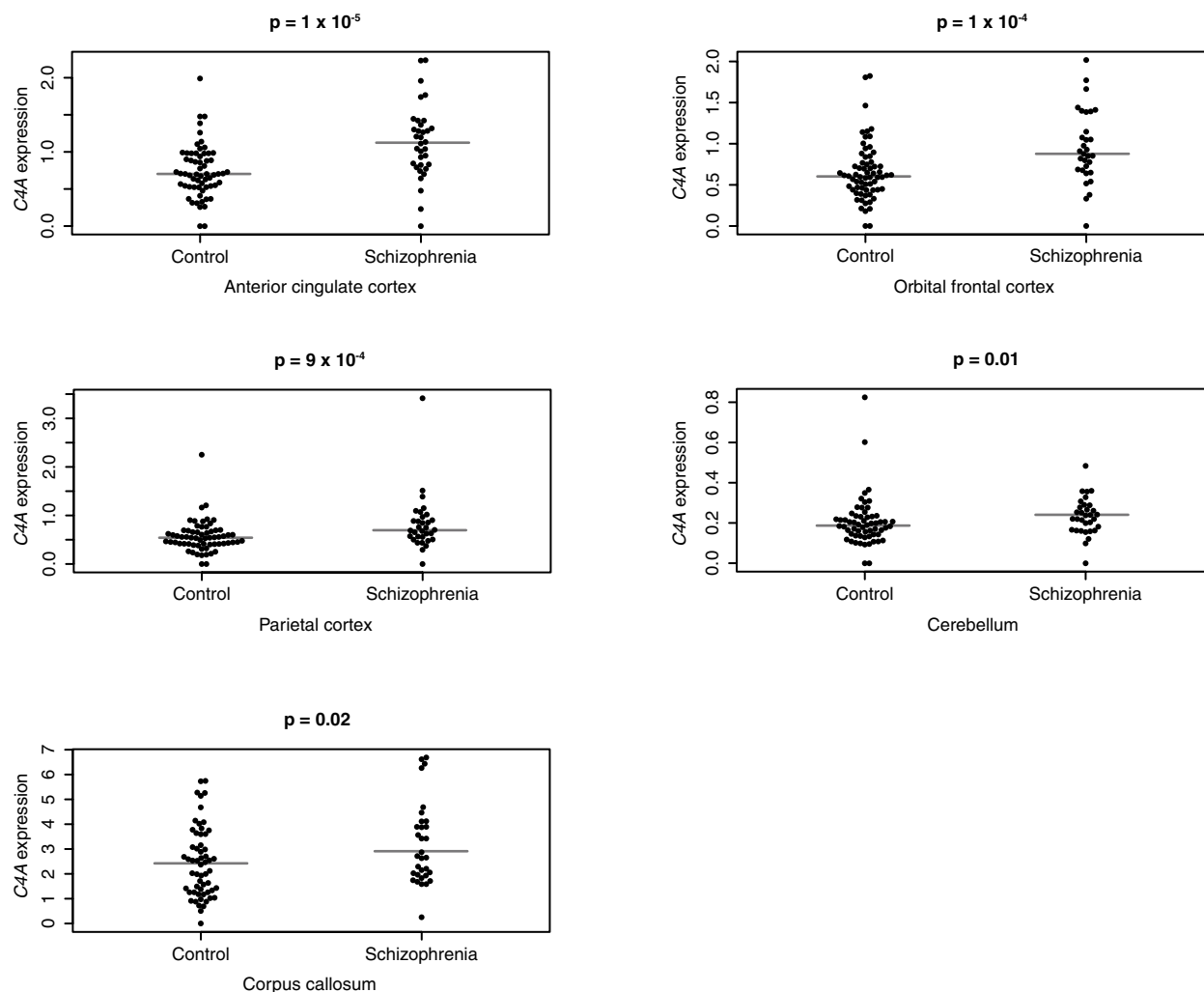
Position on chromosome 6 (Mb)

nearby SNPs, associations to other SNPs are shown in grey. The series of conditional analyses shown in **b–e** parallels the analyses in Fig. 4. Further detail on the most strongly associating *HLA* alleles (including conditional association analysis) is provided in Extended Data Fig. 7.

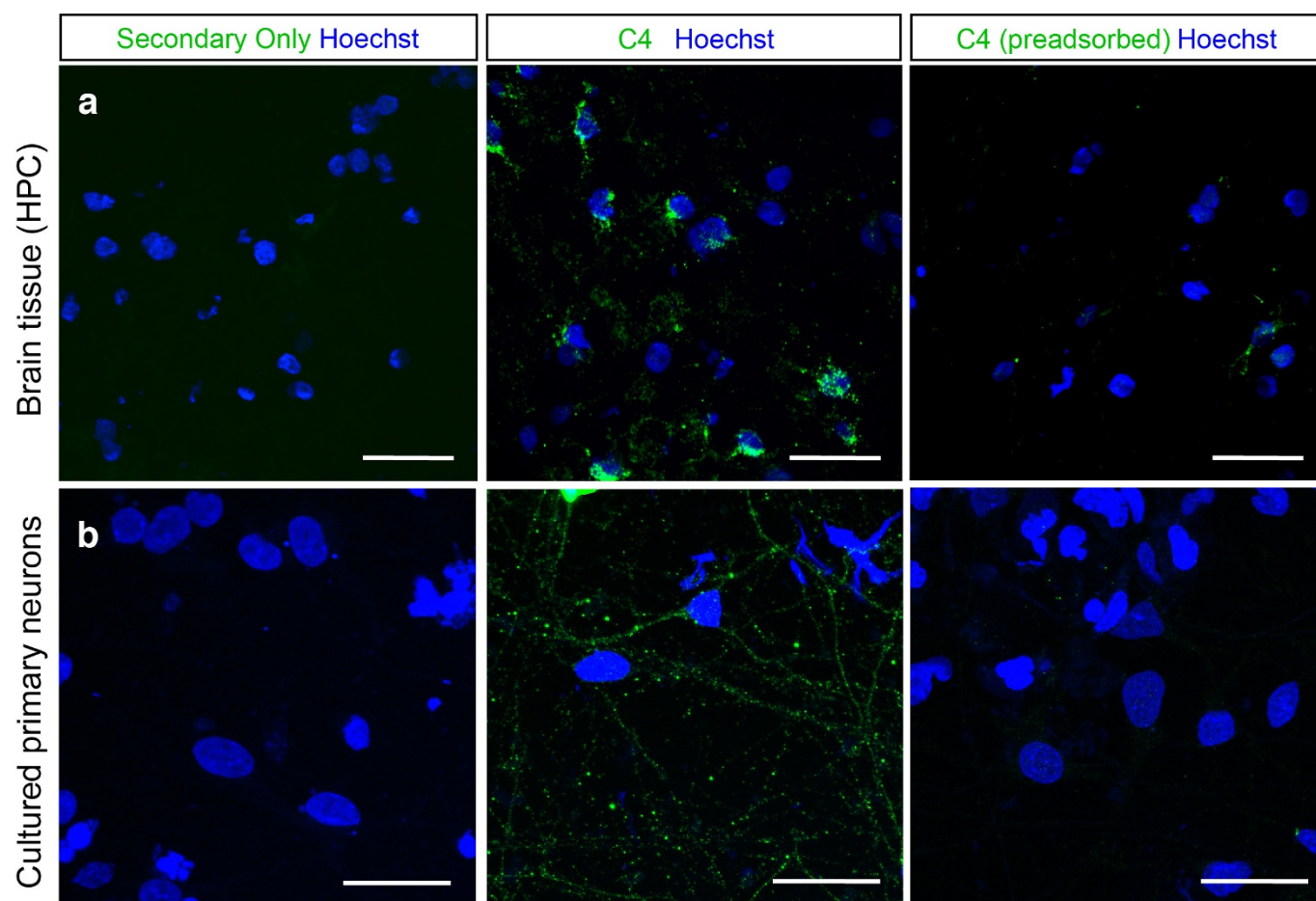
Variants included in analysis	Association p-value				
	rs13194504	Genetically predicted <i>C4A</i> expression (C4Aexp)	<i>B*0801</i>	<i>DRB1*0301</i>	<i>DQB1*02</i>
rs13194504	5.50E-28				
<i>C4Aexp</i>		3.60E-24			
<i>B*0801</i>			1.20E-21		
<i>DRB1*0301</i>				6.40E-19	
<i>DQB1*02</i>					6.25E-17
rs13194504, <i>C4Aexp</i>	8.00E-14	7.80E-10			
rs13194504, <i>B*0801</i>	5.75E-11		2.00E-04		
rs13194504, <i>DRB1*0301</i>	2.89E-15			6.20E-06	
rs13194504, <i>DQB1*02</i>	9.60E-19				1.82E-07
rs13194504, <i>C4Aexp</i> , <i>B*0801</i>	6.94E-11	8.23E-07	0.96		
rs13194504, <i>C4Aexp</i> , <i>DRB1*0301</i>	1.39E-12	2.18E-05		0.41	
rs13194504, <i>C4Aexp</i> , <i>DQB1*02</i>	3.06E-13	1.03E-04			0.03

Extended Data Figure 7 | Detailed association analysis for the most strongly associating classical *HLA* alleles. The most strongly associating *HLA* loci were *HLA-B* (in primary analyses, Fig. 4a and Extended Data Fig. 6a) and *HLA-DRB1* and *HLA-DQB1* (in analyses controlling for the signal defined by rs13194504, Fig. 4c and Extended Data Fig. 6b). At these loci, the most strongly associating classical *HLA* alleles were *HLA-B*0801*, *HLA-DRB1*0301*, and *HLA-DQB*02*, respectively. These *HLA* alleles are all in strong but partial LD with *C4* BS, the most protective of the *C4* alleles; they are also in partial LD with the low-risk allele at rs13194505,

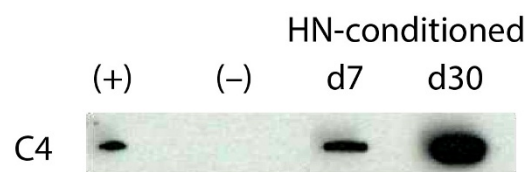
representing the distinct signal several megabases to the left (Fig. 4). In joint analyses with each of these *HLA* alleles, genetically predicted *C4A* expression and rs13194505 continued to associate strongly with schizophrenia, while the *HLA* alleles did not. In further joint analyses with rs13194504 and genetically predicted *C4A* expression, 0 of 2,514 tested *HLA* SNP, amino acid and classical-allele polymorphisms (from ref. 55, including all variants with minor allele frequency (MAF) >0.005) associated with schizophrenia as strongly as rs13194504 or predicted *C4A* expression did.



Extended Data Figure 8 | Expression of C4A RNA in brain tissue (five brain regions) from 35 schizophrenia cases and 70 non-schizophrenia controls, from the Stanley Medical Research Institute Array Consortium. C4A RNA expression levels were measured by ddPCR. *P* values are derived from Mann–Whitney *U*-test.

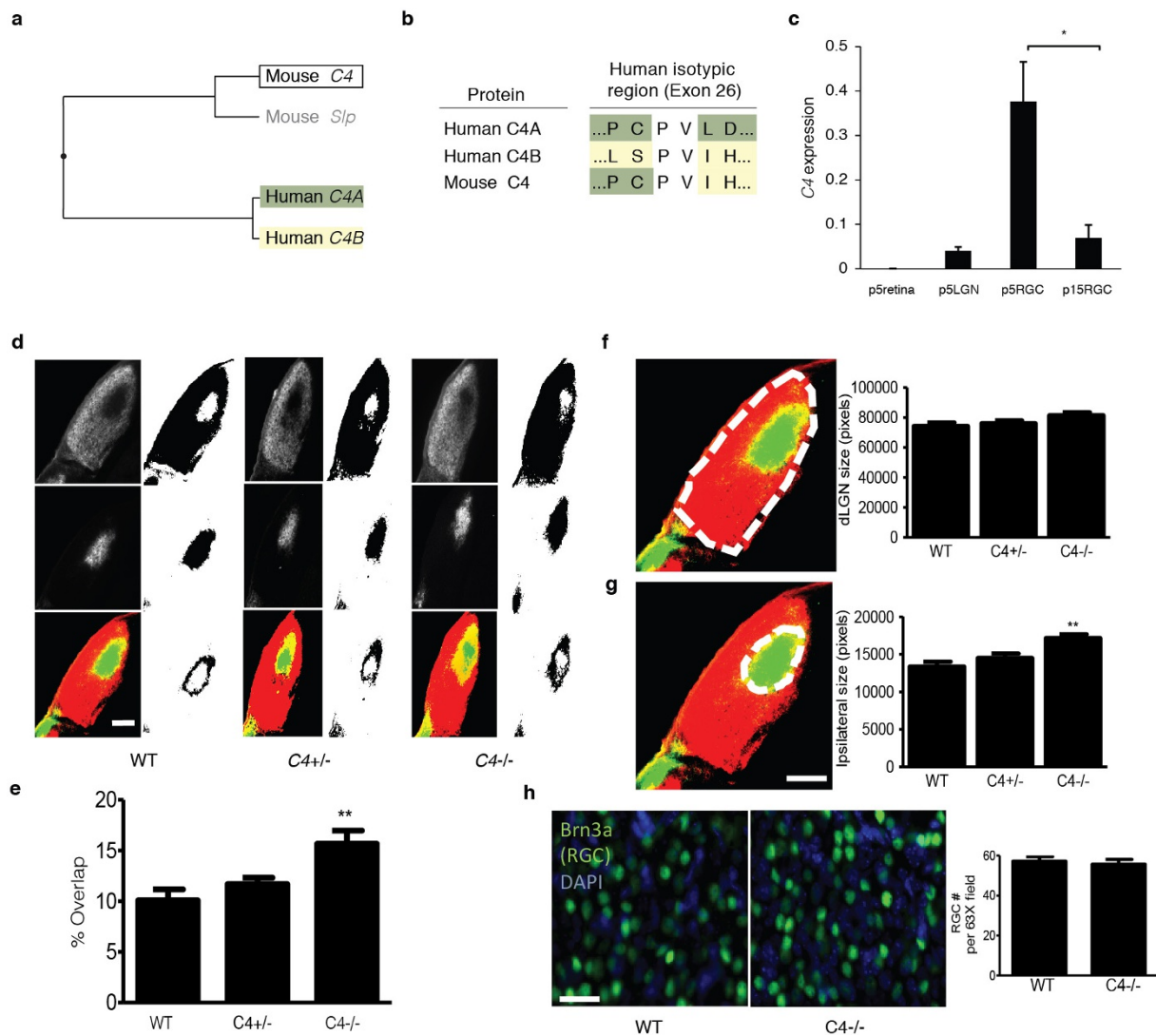


c



Extended Data Figure 9 | Secretion of C4, and specificity of the monoclonal anti-C4 antibody for C4 protein in human brain tissue and cultured primary cortical neurons. **a**, Brain tissue (from an individual affected with schizophrenia) was stained with a fluorescent secondary antibody, C4 antibody, or C4 antibody that was pre-adsorbed with purified C4 protein. Confocal images demonstrate the loss of immunoreactivity in the secondary-only and pre-adsorbed conditions. **b**, Primary human neurons were stained with a fluorescent secondary antibody, C4 antibody or C4 antibody that was pre-adsorbed with purified C4 protein. Confocal

images demonstrate the loss of immunoreactivity in the secondary-only and pre-adsorbed conditions. Scale bars, 25 μ m. **c**, Secretion of C4 protein by cultured primary neurons. Western blot for C4 protein analysis. (+) Purified human C4 protein. (-) Unconditioned medium, a negative control. HN-conditioned shows the same medium after conditioning by cultured human neurons at days 7 (d7) and 30 (d30). Details of western blot protocol, antibody catalogue numbers and concentrations used are in Supplementary Methods. C4 molecular weight, ~210 kDa.



Extended Data Figure 10 | Mouse *C4* genes and additional analyses of the dLGN eye segregation phenotype in *C4* mutant mice and wild-type and heterozygous littermate controls. **a**, The functional specialization of *C4* into *C4A* and *C4B* in humans does not have an analogy in mice. Although the mouse genome contains both a *C4* gene and a *C4*-like gene (classically called *Slp*), and these genes are also present as a tandem duplication within the mouse MHC locus, analysis of the encoded protein sequences indicates a distinct specialization, as illustrated by the protein phylogenetic tree. Top, mouse *Slp* is indicated in grey to reflect its potential pseudogenization: *Slp* is already known to have mutations at a C1s cleavage site, which are thought to abrogate activation of the protein through the classical complement pathway⁵⁶; and the *M. musculus* reference genome sequence (mm10) at *Slp* shows a 1-bp deletion (relative to *C4*) within the coding region at chr17:34815158, which would be predicted to cause a premature termination of the encoded protein. In some genome data resources, mouse *Slp* and *C4* have been annotated respectively as '*C4a*' (for example, NM_011413.2) and '*C4b*' (for example, NM_009780.2) based on synteny with the human *C4A* and *C4B* genes, but the above sequence analysis indicates that they are not paralogous to *C4A* and *C4B*. **b**, Sequence differences between *C4A* and *C4B*—which are otherwise 99.5% identical at an amino acid level—are concentrated at the 'isotypic site' where they shape each isotype's relative affinity for different molecular targets^{19,20}. At the isotypic site, mouse *C4* contains a combination of the residues present in human *C4A* and *C4B*. **c**, Expression

of mouse *C4* mRNA in whole retina and lateral geniculate nucleus (LGN) from P5 animals and in purified retinal ganglion cells (RGCs) from P5 and P15 animals. These time points were chosen as P5 is a time of more robust synaptic refinement in the retinogeniculate system compared to P15. The same assays detected no *C4* RNA in control RNA isolated from *C4*^{-/-} mice (not shown). *n* = 3 samples for p5 retina, LGN, and P15 RGCs; *n* = 4 samples for P5 RGCs; **P* < 0.05 by ANOVA with post-hoc Tukey–Kramer multiple-comparisons test. **d**, Representative images of dLGN innervation by contralateral projections (red in bottom image), ipsilateral projections (green in bottom image), and their overlap (yellow in bottom image). Scale bar, 100 μm. **e**, Quantification of the percentage of total dLGN area receiving both contralateral and ipsilateral projections shows a significant increase in *C4*^{-/-} compared to wild-type littermates (ANOVA, *n* = 5 mice per group, *P* < 0.01). These data are consistent with results using *R* value analysis as shown in Fig. 7. **f**, Quantification of total dLGN area showed no significant difference between wild-type and *C4*^{-/-} mice (ANOVA, *n* = 5 per group, *P* > 0.05). **g**, Quantification of dLGN area receiving ipsilateral innervation showed a significant increase in ipsilateral territory in the *C4*^{-/-} mice compared to wild-type littermates (ANOVA, *n* = 5 mice per group, *P* > 0.01). This result is consistent with defects in eye specific segregation. Scale bar, 100 μm. **h**, The number of RGCs in the retina was estimated by counting the number of Brn3a⁺ cells in wild-type and *C4*^{-/-} mice. No differences were observed between wild-type and *C4*^{-/-} mice (*t*-test, *n* = 4 mice per group, *P* > 0.05). Scale bar, 100 μm.